NASA/TM—2004-212947

Elevated Temperature Deformation of Fe-39.8Al and Fe-15.6Mn-39.4Al

J. Daniel Whittenberger
Glenn Research Center, Cleveland, Ohio

March 2004

The NASA STI Program Office . . . in Profile

Since its founding, NASA has been dedicated to the advancement of aeronautics and space science. The NASA Scientific and Technical Information (STI) Program Office plays a key part in helping NASA maintain this important role.

The NASA STI Program Office is operated by Langley Research Center, the Lead Center for NASA's scientific and technical information. The NASA STI Program Office provides access to the NASA STI Database, the largest collection of aeronautical and space science STI in the world. The Program Office is also NASA's institutional mechanism for disseminating the results of its research and development activities. These results are published by NASA in the NASA STI Report Series, which includes the following report types:

- TECHNICAL PUBLICATION. Reports of completed research or a major significant phase of research that present the results of NASA programs and include extensive data or theoretical analysis. Includes compilations of significant scientific and technical data and information deemed to be of continuing reference value. NASA's counterpart of peer-reviewed formal professional papers but has less stringent limitations on manuscript length and extent of graphic presentations.

- TECHNICAL MEMORANDUM. Scientific and technical findings that are preliminary or of specialized interest, e.g., quick release reports, working papers, and bibliographies that contain minimal annotation. Does not contain extensive analysis.

- CONTRACTOR REPORT. Scientific and technical findings by NASA-sponsored contractors and grantees.

- CONFERENCE PUBLICATION. Collected papers from scientific and technical conferences, symposia, seminars, or other meetings sponsored or cosponsored by NASA.

- SPECIAL PUBLICATION. Scientific, technical, or historical information from NASA programs, projects, and missions, often concerned with subjects having substantial public interest.

- TECHNICAL TRANSLATION. English-language translations of foreign scientific and technical material pertinent to NASA's mission.

Specialized services that complement the STI Program Office's diverse offerings include creating custom thesauri, building customized databases, organizing and publishing research results . . . even providing videos.

For more information about the NASA STI Program Office, see the following:

- Access the NASA STI Program Home Page at ***http://www.sti.nasa.gov***

- E-mail your question via the Internet to help@sti.nasa.gov

- Fax your question to the NASA Access Help Desk at 301–621–0134

- Telephone the NASA Access Help Desk at 301–621–0390

- Write to:
  NASA Access Help Desk
  NASA Center for AeroSpace Information
  7121 Standard Drive
  Hanover, MD 21076

NASA/TM—2004-212947

Elevated Temperature Deformation of Fe-39.8Al and Fe-15.6Mn-39.4Al

J. Daniel Whittenberger
Glenn Research Center, Cleveland, Ohio

National Aeronautics and
Space Administration

Glenn Research Center

March 2004

This work was sponsored by the Low Emissions Alternative Power Project of the Vehicle Systems Program at the NASA Glenn Research Center.

Available from

NASA Center for Aerospace Information
7121 Standard Drive
Hanover, MD 21076

National Technical Information Service
5285 Port Royal Road
Springfield, VA 22100

Available electronically at http://gltrs.grc.nasa.gov

Elevated Temperature Deformation of Fe-39.8Al and Fe-15.6Mn-39.4Al

J. Daniel Whittenberger
National Aeronautics and Space Administration
Glenn Research Center
Cleveland, Ohio 44135

Summary

The elevated temperature compressive properties of binary Fe-39.8 at%Al and Fe-15.6Mn-39.4Al have been measured between 1000 and 1300 K at strain rates between 10^{-7} and 10^{-3} s^{-1}. Although the Mn addition to iron aluminide did not change the basic deformation characteristics, the Mn-modified alloy was slightly weaker. In the regime where deformation of FeAl occurs by a high stress exponent mechanism ($n \approx 6$), strength increases as the grain size decreases at least for diameters between ~200 and ~10 μm. Due to the limitation in the grain size- flow stress-temperature-strain rate database, the influence of further reductions of the grain size on strength is uncertain. Based on the appearance of subgrains in deformed iron aluminide, the comparison of grain diameters to expected subgrain sizes, and the grain size exponent and stress exponent calculated from deformation experiments, it is believed that grain size strengthening is the result of an artificial limitation on subgrain size as proposed by Sherby, Klundt and Miller (*Met. Trans A.* **8A** (1977) 843–50).

Introduction

As part of a program to study the elevated temperature deformation characteristics of B2 crystal structure aluminides in the mid-1980's, the behavior of solid solution CoAl-based alloys containing significant amounts (~15 at%) of Fe and Ni was examined (ref. 1). Concurrent with this work, the potential of solid solution strengthening of Fe-40Al alloyed with 15 Mn was also investigated but never reported. Mn was chosen as the alloying addition because very large amounts can be added to FeAl while maintaining a single phase (refs.2 and 3), and the 1984 study by Titran, et al. (ref. 4) indicated that small Mn additions (1 or 5 at%) to FeAl produced higher 1300 K flow stresses than exhibited by the base alloy. However in the mid 1990's a few studies (refs. 5 and 7) were undertaken to determine the effect of small Mn additions on the room temperature properties of FeAl, but none of these lower temperature experiments revealed much improvement; if anything, Mn produced slight weakening of the iron aluminide at room temperature in comparison to the unalloyed compositions.

While the effects of alloying Mn on strength are uncertain, it was shown (refs. 8 to 10) that decreasing the grain size (d) could either positively or negatively affect the flow properties of FeAl at temperatures as high as 1400 K. Strengthening by grain size refinement occurred when deformation was controlled by a high stress exponent ($n \approx 6$) mechanism; however, when plastic flow was governed by the $n \approx 3$ process, mechanical strength increased with an increasing grain size. Based on mid 1980's testing (refs. 8 and 9) the high stress exponent mechanism could operate at relatively high temperatures and slow strain rates: for example, deformation of $d \geq 20$ μm alloys at 1200 K for strain rates between 10^{-5} and 10^{-7} s^{-1} is described by $n \approx 6$ (ref. 9). With the current emphasis of using FeAl-based alloys at and below 1000 K (ref. 11), strengthening by decreasing the grain size might be an effective and simple means of producing strong materials.

The following report discusses the effects of both a large Mn addition and grain size on pre-alloyed, powder metallurgy nominally Fe-40Al alloys, where the initial grain size was modified by the choice of extrusion temperature. Flow stress-strain rate-temperature behavior was determined between 1000 and 1300 K in air through constant velocity testing in compression. The results from this effort are compared with the known behavior of binary iron aluminide and its alloys.

Experimental Procedures

Prealloyed, –80 mesh gas atomized powders of Fe-39.8Al (Fe-40Al) and Fe-15.6Mn-39.4Al (FeMnAl) were purchased from Alloy Metals, Troy, MI (table I). Fully dense materials, suitable for mechanical property testing, were fabricated by hot extruding 76 mm outside diameter, 6.4-mm-thick wall steel cans which had previously been filled with about 1200 g of powder and encapsulated under vacuum. Round to round extrusions were undertaken at a 16:1 reduction ratio and several temperatures (table II). Compaction at 1505 K followed by extrusion at 1505K of FeMnAl (FeMnAl-I) was initially selected to agree with the method initially utilized for the base line binary alloy (ref. 8). As compaction was not required to obtain full density (ref. 8), the remainder of the consolidations were undertaken by direct extrusion of the powder. The lower extrusion temperatures in table II for Mn-modified iron aluminide (FeMnAl-II) and the binary iron aluminide were selected to yield a smaller as-extruded grain size (ref. 8) while maintaining the extrusion pressure beneath the press limit of 1310 MPa. To test the stability of the as-extruded grain structures, samples from the lower temperature extrusions were annealed for 16 h at the extrusion temperature +200 K: alloys Fe-40Al-ht and FeMnAl-IIht in table II.

Cylindrical test specimens 10 mm long with a 5 mm diameter were prepared by electrodischarge machining and grinding, where their length was parallel to the extrusion direction. Samples were taken from all the as-extruded aluminides and their heat treated versions (table II). Constant velocity compression tests were conducted at speeds ranging from 2.12×10^{-3} to 2.12×10^{-6} mm/s in a universal test machine between 1000 and 1300 K in air. Autographically recorded load-time charts were then converted to true compressive stresses, strains, and strain rates via the offset method and the assumption of conservation of volume. Additional details concerning specimen fabrication and test procedures can be found in (refs. 8 and 9).

Longitudinal samples were taken from the as-extruded and heat treated alloys, metalographically mounted, polished and immersion etched in a mixture of 100 ml H_2O + 20 ml HNO_3 + 3 ml HF imm to reveal the grain structure. Grain size was calculated using the circle intercept method on photomicrographs taken under Differential Interference Contrast (DIC), and the initial grain sizes of the hot extruded and heat treated alloys are given in table II. A similar technique was applied to selected compression tested samples to reveal the microstructure along the specimen length after deformation.

Results

Compressive Strength Properties

True compressive stress-strain curves from constant velocity testing as functions of temperature and nominal strain rate are presented for 1000 K as-extruded and 1000 K extruded + heated treated Fe-40Al in figures 1 and 2, respectively; and similar plots are given in figures 3 to 5 for 1505 K as-extruded FeMnAl, 1100 K as-extruded and 1100 K extruded + heat treated FeMnAl, respectively. In general both compositions exhibited two types of stress-strain plots: continuous flow at a more or less constant stress after initial working for 1 to 2 percent strain (fig. 1(a) for example) or continuous slow work hardening after the initial rapid work hardening during the first ~2 percent deformation (fig. 1(d) at nominal strain

rates of 2.2×10^{-5} and 2.2×10^{-6} s^{-1}). A much less common behavior involved yielding followed by strain softening (fig. 1(d) at 2.2×10^{-3} s^{-1} and fig. 2(a) at 2.0×10^{-4} s^{-1}, for instance). A number of duplicate tests were also undertaken, and they are denoted by the stress-strain plots utilizing solid symbols in figures 1 to 5. Repeat testing general gave very similar stress-strain curves (i.e., 1100 K deformation of Fe-40Al (figs. 1(b) and (c)) and FeMnAl-I (fig. 3(a) at the two slowest strain rates). The one exception was duplicate testing of Fe-40Al at 1200 K to 2.2×10^{-6} s^{-1} (fig. 1(c)) where one experiment produced continuous work hardening and the other continued flow at a more or less constant stress.

Based on the stress-strain curves in figures 1 to 5, the strength of any material depended on the temperature and imposed deformation rate, where for any particular deformation rate the strength decreased as the temperature was increased and at any constant temperature strength decreased with a decreasing strain rate.

True compressive flow stress (σ)-strain rate ($\dot{\varepsilon}$)-temperature (T) plots are presented in figure 6 for the two forms of Fe-40Al and in figure 7 for the three different versions of FeMnAl. The data points in these figures represents the flow stress and strain rate determined at 3 percent strain from each stress-strain plot in figures 1 to 5. Where appropriate, the data were fitted to the standard temperature compensated-power law equation by multiple linear regression techniques

$$\dot{\varepsilon} = A\,\sigma^{n}\exp(-Q/(RT)), \tag{1}$$

where A is a constant in s^{-1}, n is the stress exponent, Q is the activation energy for deformation, and R is the universal gas constant. The range of each fit was chosen to be as broad as possible in $\dot{\varepsilon}$-σ-T space consistent with a good visual appearance and a relatively high coefficient of determination ($R_d^2 > 0.95$). The results of these fits in terms of n and Q values and their standard deviations (δ_n and δ_Q) as well as the coefficients of determination (R_d^2) are given in table III(a). The curves in each part of figures 6 and 7 indicated the extent of each fit.

Fitting of the Fe-40Al results indicated that the behavior fell into two distinct regimes (fig. 6(a)), where at the lower temperatures (1000 +1100 K) deformation occurred by a high stress exponent mechanism ($n \approx 6.6$, table III(a)), while at the higher temperatures plastic flow was described by a much lower stress exponent ($n \approx 4.2$) . The heat treated form of Fe-40Al (fig. 6(b)) exhibited an intermediate stress exponent (~4.9) between 1000 and 1200 K; whereas the 1300 K properties were much less dependent on stress ($n = 2.7$). In spite of the difference in the stress exponents between the two groups, both had the same activation energy for deformation of ~410 kJ/mol.

Statistical comparison of the flow stress-strain rate-temperature data for the two forms of Fe-40Al utilizing a dummy variable indicated that within the current limits of testing there was very little difference in strength between either the as-extruded or heat treated materials, and the results could be successfully joined to give two groups: (1000 +1100 K) and (1200 +1300 K). This joining (table III(b)) lead to behaviors which basically followed as-extruded Fe-39.8Al, where (1000 +1100 K) group displayed a high stress exponent ($n = 6$) while the (1200 +1300 K) group compressed per $n = 3.8$.

In only one case did fitting of the compression data for the Mn-modified iron aluminide to equation (1) lead to a relatively high stress exponent, where $n = 5.5$ for 1100 K as-extruded FeMnAl-II tested between 1000 and 1200 K (table III(a)). All the other versions of Fe-15.6Mn-39.4Al exhibited plastic flow by much lower stress exponent mechanisms ($n < 4.3$). In terms of the activation energies for deformation, the two as-extruded FeMnAl alloys displayed values of about 430 kJ/mol which is similar to the Q's for Fe-40Al (table III(a)). The heat treated alloy (FeMnAl-IIht), however, possessed a much lower activation energy of about 335 kJ/mol.

Both visually and statistically the 1505 K extruded FeMnAl-I (fig. 7(a)) is weaker than the 1100 K extruded version (fig. 7(b)) between 1000 and 1200 K. The same is true in a statistical sense for the 1300 K flow stress-strain rate behavior, but in reality the strength difference between 1505 and 1100 K

as-extruded FeMnAl is small. This contention is a result of the fit to equation (1) for the joined 1300 K FeMnAl-I and FeMnAl-II data sets with a dummy variable to represent each material which indicated that the higher temperature extruded alloy is slightly weaker (table III(b)).

Statistical and visual (figs. 7(b) and (c)) contrasting of the 1000 to 1200 K flow stress-strain rate data for 1100 K extruded Fe-15.6Mn-39.4Al (FeMnAl-II) and its 16 h at 1300 K heat treated form (FeMnAl-IIht) indicated that within the current limits of testing that the hot extruded material was stronger than the heat treated version. However at 1300 K both forms statistically had the same strength which could be described by one equation (table III(b)).

Post Compression Microstructure

Because of the relative weakness of FeMnAl-I, it was only examined in the as-extruded form which showed a grain size of about 100 μm (table II). Untested and tested samples of the lower temperature extruded and heat treated forms of Fe-40Al and FeMnAl were metallographically studied in more detail. The unstressed annealing of Fe-40Al for 16 h at 1200 K essentially did not produce grain growth; however the 16 h to 1300 K heat treatment of FeMnAl-II produced about a 50 percent increase in the average grain size (table II). Representative photomicrographs of compression tested Fe-40Al and FeMnAl are presented in figures 8 and 9, respectively, and table IV shows the measured grain size as a function of the nominal deformation conditions. In this study the samples deformed at 2.2×10^{-4} s^{-1} were subjected to about 25 percent true strain (±2 percent); whereas the specimens deformed at slower rates, with a couple of exceptions, were only deformed about half as much.

Fe-40Al, FeMnAl-II and FeMnAl-IIht appear to have maintained their original grain sizes (table II) during 1000 K testing and the fastest rate at 1100 K (table IV and figs. 8(a), 9(a), and 9(c)); whereas the grain size of Fe-40Al-ht increased about 50 percent from its original diameter (6.5 to ~10 μm) under the same deformation conditions (table IV and fig. 8(c)). With the exception of 1000 K testing, in general as the time at temperature increased (decreasing strain rates), the grain sizes of all four materials grew (table IV, figs. 8(b), 8(d), 9(b), and 9(d)) compared to their original sizes, but the growth was limited to a factor of ~3 in the worst case (FeMnAl-II from 6.5 μm to 18.5 μm after 1300 K to 2.2×10^{-7} s^{-1} to 10 percent deformation (fig. 9(b)).

Discussion

Alloying With Mn

Since the strength for the 6.5 μm grain size 1100 K extruded FeMnAl-II (fig. 7(b)) is greater than that of the 100 μm grain size 1505 K densified alloy (FeMnAl-I, fig. 7(a)), it can be concluded that grain size can influence the elevated deformation properties of Fe-15Mn-40Al as is the case of binary iron aluminides (refs. 8 to 10). Therefore a direct comparison of the strength levels of 5.5 μm Fe-40Al (fig. 6(a)) to that of 100 μm FeMnAl-I (fig. 7(a)) to determine the influence of replacing 15 percent Fe with Mn would not be reasonable. On the other hand, the influence of Mn can be assessed from the combined Fe-40Al + FeMnAl-II data since the starting forms all three possess about a 6 μm grain size (table II). Visual contrasting of these results can be made in figure 10, where the FeMnAl-II data points (fig. 7(b)) are compared to the predicted behavior of joined Fe-40Al + Fe-40Al-ht (table III(b)), and it suggests that the unmodified aluminide is stronger. This contention was tested by multiple linear regression fitting with dummy variables, and the analyses (table III(b)) confirmed that substitution of about 15 at% Mn for Fe slightly weakens Fe-40Al between 1000 and 1300 K. Because the stress exponent was decreasing with

temperature, three separate fits were required to best describe the data: (1000 + 1100 K), 1200 and 1300 K. The descriptions in table III(b) indicate that the Mn addition did not affect the basic deformation mechanisms of the iron aluminides; instead the Mn just slightly increased the pre-exponential term of eq. (1) by a factor of ~2. Thus the conclusion to be drawn from figure 10 and the regression analysis in table III(b) is that alloying FeAl with relatively large amount of Mn does not produced the desired elevated temperature hardening.

Grain Size Strengthening

Even though a Mn addition did not improve strength, it was believed (refs. 8 to 10) that reducing the grain size below 10 μm would result in a strength improvement in B2 iron aluminide. Although strength orders with decreasing grain size for the 185, 55, and 10 μm versions of Fe-39.8Al (ref. 8) at 1200 K (fig. 11(a)), the ~10 and ~6 μm forms of Fe-39.8Al have about the same resistance to deformation. The expectation of grain size hardening at 1200 K for small diameters (<20 μm) was probably unwarranted since the deformation for such grain sizes occurs by a stress exponent <4 mechanisms (ref. 8, table II(b)); whereas grain structure controlled strengthening was only observed during $n \approx 6$ plastic flow (ref. 9). While the data does not exist to make a direct comparison of the strength of Fe-39.8Al as a function of grain size at lower test temperatures (fig. 11(b)) contrasts the behavior of two nominally 40 μm Fe-48Al alloys to the present ~6 μm Fe-39.8Al (Fe-40Al) at 1100 K. Because it was shown that Al content between 48.7 and 39.8 at% has no effect on the 1200 to 1400 K strength of FeAl (ref. 9), the difference in composition among the alloys in figure 11(b) is believed to be immaterial. With this assumption, it is clear in this figure that decreasing the grain size can improve the strength of FeAl at 1100 K.

Based on figure 11(b) and reference 9, the flow strength-strain rate-temperature-initial grain size data from the $n \approx 6$ regime for iron aluminide alloys containing between 48.7 and 39.8 at% Al from this work and (refs. 8 and 9) were fitted to eq. (1) and

$$\dot{\varepsilon} = Bd^{p}\sigma^{n}\exp(-Q/(RT)), \tag{2}$$

where B is a constant in s^{-1} and p is the grain size exponent. For purposes of documentation the compositions of the alloys, initial grain sizes and temperature-flow strength-strain rate data used in conjunction with eq. (2) are given in appendix A. Results for these fits are given in table V, where δ_p is the standard deviation of the grain size exponent. Irrespective of whether the data from all the compositions or only the Fe-39.8Al results were considered, similar behavior was observed. Namely the use of the temperature compensated power law (eq. (1)) alone gave a poor fit compared to eq. (2) with its additional grain size term; however the term d^p by itself was not able to explain all the grain size dependency. This conclusion resulted from the use of a dummy variable in the analyses based on initial grain size (i.e., $X = 0$ for grain sizes greater than or equal to 9 μm, and $X = 1$ for grain sizes less than 9 μm). While the fits using the dummy variable produced a only small increase in the coefficient of determination (table V, ~0.95 from ~0.93), the t-statistic and F-statistic for the dummy variable were significant at the 1 percent level (for all compositions of B2 iron aluminide: $t = 6.37$, $F = 40.2$ and for only the Fe-39.8Al results: $t = 4.03$, $F = 16.3$). For completeness it should be noted that like increases in R_d^2 can be obtained from the data and eq. (2) using dummy variables to give either two stress exponents (n_1 for grain sizes greater than or equal to 9 μm, and n_2 for grain sizes less than 9 μm) or two activation energies (Q_1 for grain sizes greater than or equal to 9 μm, and Q_2 for grain sizes less than 9 μm). Extending the analyses beyond either two pre-exponential terms, two stress exponents or two activation energies did not statistically improve the fit.

As there was little difference among the fits involving either two pre-exponential terms, two stress exponents or two activation energies, the grain size dependent pre-exponential fit is given below and in table V as it allows an easy demonstration of competing grain size behaviors, where

$$\dot{\varepsilon} = \exp(9.055+1.87X^{*})d^{2.48}\sigma^{5.86}\exp(-(448.7/(RT)). \quad (3)$$

$^{*}X = 0$ for the grain sizes ≥9 μm and $X = 1$ for grain sizes <9 μm

The ability of this equation to predict strength is illustrated by the two curves in figure 11(b) for 40, and 6 μm grain size iron aluminides at 1100 K. Because the extra term in the pre-exponential constant for grain sizes less than 9 μm is positive, the value of the pre-exponential in eq. (3) is increased by a factor of ~6.5 which, in turn, means that strength of iron aluminide with grain sizes <9 μm would be less than expected based on larger grain diameters.

While it is clear that decreasing the grain size can strength iron aluminides at T<1200 K (fig. 11(b)), it is not currently possible to demonstrate from the existing data for binary iron aluminide alloys that strength monotonically increases as the grain size decreases below 9 μm or that the strength continues to decrease for grain sizes greater than 200 μm. Resolution of this question will require measurement of the 1000 and 1100 K strength properties of Fe-39.8Al with initial grain sizes >7 μm and/or 1000 and 1100 K properties for other compositions of FeAl with a large range of grain sizes.

Given that grain size reduction can improve strength of binary FeAl at 1100 K (refs. 9 and 10, fig. 11(b)), is the improvement significant? Table VI compares the predicted 1073 K behavior of FeAl for several grain sizes to the strength levels of several multi-element alloyed iron aluminide alloys which contain both solid solution strengthening additions (Mo,Ti,Zr) as well as elements designed to promote precipitation hardening (C, B). These results indicate that alloying can produce nominally 1073 K to 5×10^{-4} s^{-1} strength levels in the 100 to 150 MPa range, but such values can also be achieved in binary FeAl through grain size reduction to 10 μm. Most interesting is the data from Maziasz et al. (ref. 14), who observed that decreasing the grain size of a complex alloy (Fe-38.5Al-0.2Mo-0.05Zr-0.13C) significantly increased the strength. This suggests that both alloying and grain size strengthening mechanisms can be superimposed.

The probable source for grain size strengthening in FeAl comes from the restriction in the size of subgrains being formed during deformation per Sherby, Klundt and Miller (ref. 15). Since this type of restricted subgrain size strengthening has been observed in small grain sized NiAl (ref. 16), it is logical that, if subgrains form during elevated temperature straining in iron aluminide, their maximum diameter must be limited to the grain size. If this is the case in FeAl, then the elevated temperature strain rate would be given by

$$\dot{\varepsilon} = Bd^{3}\sigma^{n'}\exp(-Q/(RT)), \quad (4)$$

where the grain size exponent would be three and the stress exponent n' equals the basic stress exponent for FeAl plus 3 ($n_b + 3$) (refs. 15 and 16). Simple examination of eq. (3) indicate that the current calculated grain size exponent for FeAl is close to three.

Since the 1980s investigations of binary FeAl, where grain size strengthening was observed and the existence of subgrains via light optical microscopy evidence presented (refs. 8 and 9), a number of other studies have demonstrated the formation of subgrains during elevated temperature deformation (refs. 17 to 20). Lin et al. (refs. 17 and 18) extensively studied the misorientation of the subboundaries in Fe-36.5Al and Fe-36.5Al-2Ti alloys deformed at 1173 and 1273 K. Reiman and Sauthoff (ref. 19) also indicated that subgrains were formed during testing of both very large grain sized (>1mm^3) and [001]-oriented single crystalline forms of various iron aluminides (compositions ranging from Fe-40Al to Fe-52Al) between 973 and 1273 K. Additionally, Pang and Kumar (ref. 20) presented transmission

electron photomicrographs (figs. 13(c) and (d) in ref. 21) of a Fe-40Al-0.7C-0.5B alloy tested to failure at 873 K to 10^{-2} s^{-1} which has well defined ~1 μm sugbrain substructure.

Previously, Raj and Pharr (ref. 21) have shown that the unrestricted, equilibrium subgrain size λ formed in a large variety of materials is given by

$$\lambda = 23Gb/\sigma \approx 8.8Eb/\sigma, \tag{5}$$

where G is the shear modulus, b is the magnitude of the burgers vector, and E is the elastic modulus. This equation along with Harmounche and Wolfenden's measured values of the Young's modulus for FeAl (ref. 22) described by

$$E(\text{GPa}) = 287.75 - 0.0219\text{T} - 0.0035(\text{at\% Al})^2 + 0.00305\text{T}(\text{at\% Al}) \tag{6}$$

permits the equilibrium subgrain size in FeAl to be predicted as functions of temperature, composition and applied stress. An example of such a prediction is given in figure 12(a) by the solid black line for Fe-40Al deforming by $\boldsymbol{b}$ = [001] dislocations at 1100 K along with the limit curves (gray lines) corresponding to probable error (a factor of 2) in the estimates (ref. 21). As a point of reference, per eq. (6) which indicates that the modulus is a function of both temperature and composition, increasing the temperature by 100 K would decrease the equilibrium subgrain size by ~5 percent; on the other hand increasing the Al level to 46 percent, which gave the maximum values of modulus (ref. 22), would increase the equilibrium subgrain size by ~10 percent.

Some confidence in the subgrain size predictions in figure 11(a) can be gotten from Pang and Kumar's (ref. 20) nominal 1 μm subgrain grain size after 873 K deformation, where the estimated strength value (873 K 0.2 percent yield strength of ~400 MPa and more than 50 percent tensile elongation, fig. 9, ref. 20) just prior to failure is about 600 MPa. Neglecting any influence of carbides and borides on the subgain structure, these strength and temperature conditions in combination with eqs. (5) and (6) predict that the equilibrium subgrain size would be ~0.8 μm. This value agrees closely with observation (ref. 20); hence the 1100 K predictions of the equilibrium subgrain sizes for FeAl in figure 12(a) are believed to be realistic

As subgrains form during elevated temperature deformation of B2 iron aluminide (refs. 17 to 20), it is possible for grain size strengthening to occur, and figure 12 (a) allows estimates of the grain sizes where such hardening is possible. For example if the grain size was 9 μm (horizontal dashed line in fig. 12(a)), the maximum subgrain diameter that could form would be 9 μm; thus deformation at stress levels <50 MPa (left side of dashed vertical line, fig. 12(a)) would occur under conditions where the subgrain size is limited to the grain size and extra strengthening should occur. Conversely, if deformation occurs at stress >50 MPa (right side of dashed vertical line, fig. 12(a)), the subgrains would be less than 9 μm in size, and no extra strengthening takes place. Of course such transition stresses would be very sensitive to the exact dependency between the equilibrium subgrain size in FeAl and applied stress; thus per the factor of 2 limit curves in figure 12(a), the transition stress for a 9 μm subgrain sized could vary from ~25 to ~100 MPa.

The available 1100 K flow stress-initial grain size results for both binary iron aluminides and FeMnAl-II which possessed high stress exponents ($n \approx 6$) are compared to the 1100 K predicted equilibrium subgrain size and its factor of 2 higher limit line for Fe-40Al in figure 12(b). For each grain size the far left data point signifies the measured flows stress from ~2×10^{-7} s^{-1} testing, and each subsequent data point to the right represents the flow stress at a one order of magnitude faster deformation rate. As all the flow stress data for grain sizes less than 40 μm lie to the right or are very close to the upper limit for predicted subgrain size, these grain sizes could be capable of restricting the subgrains from achieving their equilibrium diameters during deformation.

The possibility of a grain structure limiting the size of subgrains during deformation can also be shown at higher temperatures, as is illustrated in figure 12(c) at 1300 K. This figure compares the predicted 1300 K equilibrium subgrain size and its factor of 2 higher limit line for Fe-40Al to the measured flow stress for a number of different FeAl alloys. The binary aluminide compositions, initial grain sizes and strain rate ranges for the data points in figure 12(c) are given in the table which is part of the figure caption. Again in figure 12(c) for each grain size, the far left hand data point represents the flow stress measured for the slowest strain rate per the table, and each subsequent data point to the right represents the flow stress at an order of magnitude faster deformation rate. As the majority of the flow stresses for each grain size are within the regime where subgrain diameters would be limited by the grain size (i.e., eq. (5) is not obeyed), it is clearly possible for the grain structure to impose an artificial limit on the deformation subgrain size.

Per the description of eq. (4), when the subgrain size is artificially controlled, the measured stress exponent n' becomes three units higher than the basic stress exponent (ref. 15). This seemed to be the case for iron aluminide as it was noted in 1986 (ref. 9) that grain size strengthening only occurred in the high stress exponent regime ($n \approx 6$) but not when the low stress exponent mechanism ($n < 4$) was controlling. Since this early observation, other studies of the elevated deformation of FeAl have been completed. Reiman and Sauthoff's (ref. 19) compression of large grain size polycrystalline and [001]-oriented binary FeAl single crystals between 973 and 1273 K gave stress exponent values generally between 4 and 5. Sastry, Prasad and Deevi's testing of 22 μm Fe-39.6Al-0.2Mo-0.1Zr-0.4C-0.02B (ref. 12) between 1073 and 1423 K report that the stress exponent decreased with increasing temperature from $n = 7$ at 1073 K to $n = 4$ at 1373 K. Lastly, as given by the joined fits of Fe-40Al and Fe-40Al-ht data in table III(b), the stress exponent for ~6 μm Fe-40Al changes from about 6 at 1000 and 1100 K to less than 4 at 1200 and 1300 K. Taken together, it appears that basic elevated temperature deformation mechanism in FeAl occurs by an stress exponent of ~ 4 mechanism, but when some means of restricting subgrain size is introduced, the apparent stress exponent increases to 6 or more, in basic agreement with eq. (4) (ref. 15).

While deformation in iron aluminides does involve the formation of subgrains which can affect the motion of dislocations, the thermally activated process in control is very much in question. Essentially every study of elevated temperature plastic deformation (refs. 8, 9, 12, and 17 and table III) reports activation energies for deformation that range from 340 to 550 kJ/mol. Reiman and Sauthoff (ref. 19) also report a 400 kJ/mol activation energy for deformation for Fe-40Al single crystals; however they indicate a tendency for Q to decrease with increasing Al content at stresses <10 MPa such that activation energies of ~200 kJ/mol are reported for Fe-48.7Al. This was not the case for testing of polycrystalline binary FeAl alloys (refs. 8 and 9) where very high activation energies were calculated for all compositions between 39.8 and 48.7 Al irrespective of the stress levels (~150 to ~0.7 MPa) or the stress exponents ($7.5 < n < 3$).

To date diffusion studies in binary FeAl (refs. 23 and 24) have shown that the rates of diffusion are nearly independent of Al content, and they report much lower activation energies than those obtained from deformation experiments. Mehrer, et al. (ref. 23) measured tracer diffusion coefficients in Fe-26.5Al, Fe-34Al and Fe-50Al using ^{59}Fe and ^{114m}In (in place of an Al tracer) between 700 and 1500 K and determined the tracer diffusion coefficients (D^*) in the B2 phase could be described by

$$D^* \text{ for } {}^{59}\text{Fe } (\text{m}^2/\text{s}) = 5.3\times10^{-3} \exp(-265/(RT)) \text{ and}$$
$$D^* \text{ for } {}^{114}\text{In } (\text{m}^2/\text{s}) = 6.4\times10^{-3} \exp(-258/(RT)), \quad (7)$$

where the activation energies for diffusion are in kJ/mol. Nakamura, et al. (ref. 24) measured interdiffusion in alloys containing from ~40 to ~48Al between 1073 K to 1475 K and calculated the interdiffusion coefficient ($\tilde{D}$) in B2 FeAl to be about

$$\tilde{D} \ (\text{m}^2/\text{s}) = 8.4\times10^{-3} \exp(-256/(RT)) \quad (8)$$

Comparison of eqs. (7) and (8) reveals a very close agreement between interdiffusion and tracer diffusion coefficients, but these activation energies are ~150 kJ/mol less that the values from plastic flow experiments (refs. 8, 9, 12, 17, and 19 and this study).

One possible reason for the activation energy discrepancy could be due to neglecting the influence of modulus as a function of temperature in eq. (2); however, utilization of σ/E term instead of σ in this equation did not significantly change the activation energy for deformation, where

$$\dot{\varepsilon} = \exp(73.71 + 0.88X^{*})d^{2.23}(\sigma/E)^{5.68}\exp(-394.1/(RT)), \quad (9)$$

$^{*}X = 0$ for the grain sizes ≥9 μm and $X = 1$ for grain sizes <9 μm

with $R_d^2 = 0.924$ which is less than that for eq. (3) Although this approach lowered the activation energy for deformation by ~50 kJ/mol compared to eq. (3), it is still about 50 percent greater than the activation energy for diffusion (eqs. (7) and (8)). Thus, the current modulus correction approach does not appear to be successful; however it is possible that this normalization technique could still be reasonable if better modulus data were available. The E values (eq. (6)) of Harmounche and Wolfenden (ref. 22) were only measured to 1123 K which meant that considerable extrapolation was necessary to calculate the 1300 and 1400 K stress/modulus terms.

As has been recently proposed (ref. 25), it is possible that a wide band of activation energies exists which give almost as good a description of behavior as the "best" activation energy determined by multiple linear regression techniques. With this logic in mind, the flow stress-strain rate-temperature-grain size data were refitted to eq. (2) with Q force to be 260 kJ/mol per eqs. (7) and (8) which gave

$$\dot{\varepsilon} = 2.68\times10^{-2}\, p^{1.90}\, \sigma^{4.47}\, \exp(-260/(RT)) \quad (10)$$

where the R_d^2 was 0.877 and the pre exponential term was independent of grain size. While eq. (10) is simpler than eq. (3), its ability to describe the original data is much worse; thus the use of the activation energy for diffusion in iron aluminide to characterize elevated temperature deformation does not appear to be appropriate.

As neither the modulus correction (eq. (9)) nor the forcing (eq. (10)) were able to reconcile the large difference between deformation and diffusion activation energies, the reason(s) for such a huge difference between these activation energies in B2 iron aluminide is not known.

Summary of Results

The effect of a large Mn addition and grain size on the elevated temperature compressive properties of B2 crystal structure iron aluminides has been investigated. While replacement of ~15 at% Fe with Mn to produce Fe-15.6Mn-39.4Al did not change the 1000 to 1300 K deformation characteristics, the Mn-rich alloy was slightly weaker than Fe-39.8Al. Examination of the properties of binary FeAl alloys as a function of grain size reconfirmed that in the high stress exponent deformation regime ($n \approx 6$) strength increases as the grain size decreases for diameters between ~200 and ~10 μm. However within the limits of the current data base, a further reduction of the grain size for Fe-39.8Al to 6 μm did not appear to promote additional strengthening beyond that achieved at 9 μm. Consideration of the microstructure, equilibrium subgrain sizes and deformation parameters of deformed alloys indicate that grain size strengthening in FeAl is due to an artificial limitation on the sizes of subgrains, as proposed by Sherby, Klundt and Miller (ref. 15).

References

1. J. Daniel Whittenberger, *Mater. Sci. Eng*. **85** (1987) 91–99.
2. D.E. Okpalugo and J.G. Booth, *J. Phys. F. Met. Phys*. **15** (1985) 2025–2039.
3. I. Omari, A.S. Saleh, and S.H. Mahmood, *J. Magnetism and Magnetic Materials* **78** (1989) 183–189.
4. R.H. Titran, K.M. Vedula, and G.G. Anderson, High-Temperature Ordered Intermetallics Alloys MRS Proceedings **39**, Materials Research Society, Pittsburgh, PA, 1984. pp. 309–317.
5. C.H. Kong and P.R. Munore, *Scripta Metal. et Mater*. **30** (1994) 1079–83.
6. J.H Schneibel, E.P. George, E.D. Specht, and J.A. Horton, High-Temperature Ordered Intermetallics Alloys VI MRS Proceedings **364**, Materials Research Socienty, Pittsburgh, PA, 1995. pp. 73–78.
7. J.H Schneibel, E.D. Specht, and W.A. Simpson, *Intermet*. **4** (1996) 581–3.
8. J. Daniel Whittenberger, *Mat. Sci. Eng.* **57** (1983) 39–47.
9. J. Daniel Whittenberger, *Mat. Sci. Eng.* **77** (1986) 103–13.
10. J. Daniel Whittenberger, NASA TM–101382, 1988.
11. R.S.Sundar and S.C. Deevi, *Mat. Sci. Eng. A* **357** (2003) 124–33.
12. D.H. Sastry, Y.V.R.K. Prasad, and S.C. Deevi, *Mat. Sci. Eng. A* 299 (2001) 157–63.
13. J. Daniel Whittenberger, Michael V. Nathal, and Darrell J. Gaydosh. *Intermetallics* **2** (1994) 193–200.
14. P.J. Maziasz, G.M. Goodwin, D.J. Alexander, and S. Viswanathan, Proceedings of the International Symposium on Nickel and Iron Aluminides: Processing, Properties and Applications, (eds. S.C. Deevi, P.J. Maziasz, V.K. Sikka, and R.C. Cahn) ASM International, Materials Park, OH, 1997, pp. 157–176.
15. O.D.Sherby, R.H. Klundt, and A.K. Miller, *Met. Trans A*. **8A** (1977) 843–50.
16. J. Daniel Whittenberger, *J. Mat. Sci.* **22** (1987) 394–402.
17. Dongliang Lin, Dingqiang Li, and Yi Liu, *Intermetallics* **6** (1998) 243–56.
18. Dongliang Lin and Yi Liu *Mater. Sci. Eng*. **A268** (1999) 83–89.
19. U. Reimann and G. Sauthoff, *Intermetallics* **7** (1999) 437–45.
20. L. Pang, S.M. Han, and K.S. Kumar, *Acta Mater*. **50** (2002) 3623–39.
21. S.V. Raj and G.M. Pharr, *Mater. Sci. Eng*. **81** (1986) 217–237.
22. M.R. Harmouche and A. Wolfenden, *Mater. Sci. Eng*. **84** (1986) 35–42.
23. H. Mehrer, M. Eggersmann, A. Gude, M. Solamon, and B. Sepiol, *Mater. Sci. Eng*. A **A239–40** (1997) 889–98.
24. R. Nakamura, K. Takasawa, Y. Yamazaki, and Y. Iijima, *Intermetallics* **10** (2002) 195–204.
25. J. Daniel Whittenberger, R. Noebe, and R. Darolia: *Mater. Sci. Eng*. A **A367** (2004) 143–51.

TABLE I.—COMPOSITIONS (WT%) OF THE
PRE-ALLOYED FEAL POWDERS

ID	Al	C	H	Mn	N	O
Fe-40Al	24.22	0.0006	0.0006	------	0.0007	0.025
FeMnAl	24.01	0.009	0.002	19.40	0.0042	0.022

TABLE II.—THERMOMECHANICAL PROCESSING CONDITIONS
AND GRAIN SIZES FOR INTERMETALLIC ALLOYS

ID	Compaction	Extrusion	Heat treatment	Time, hr	Grain size, μm
	Temperature, K				
Fe-40Al	-----	1000	-----	---	5.5
Fe-40Al-ht	-----	1000	1200	16	6.5
FeMnAl-I	1505	1505	-----	---	100
FeMnAl-II	-----	1100	-----	---	6.5
FeMnAl-IIht	-----	1100	1300	16	9.5

TABLE III.—TEMPERATURE COMPENSATED POWER LAW DESCRIPTIONS OF THE FLOW STRESS-STRAIN RATE-TEMPERATURE BEHAVIOR FOR IRON ALUMINIDES.

Identification	Temperature range, K	A, s^{-1}	n	δn	Q, kJ/mol	δ_Q, kJ/mol	R_d^2
(a) Individual fits							
Fe-40Al	1000 to 1100	3.33×10^{3}	6.62	0.29	414.2	30.3	0.985
	1200 to 1300	1.36×10^{7}	4.18	.20	402.9	40.1	0.986
Fe-40Al-ht	1000 to 1200	8.40×10^{6}	4.85	0.29	415.3	30.6	0.969
	1300	5.49×10^{-8}	2.71	.23	------	-----	0.993
FeMnAl-I	1000 to 1300	2.87×10^{8}	4.33	0.15	410.5	13.8	0.986
FeMnAl-II	1000 to 1200	1.98×10^{8}	5.49	0.28	460.3	28.6	0.974
	1300	3.45×10^{-8}	3.26	.22	------	-----	0.986
FeMnAl-IIht[a]	1000 to 1300	7.29×10^{5}	3.51	0.22	334.9	23.9	0.957
(b) Combined fits							
Fe-40Al +	1000 to 1100	4.00×10^{5}	6.01	0.32	432.5	35.3	0.957
Fe-40Al-ht	1200 to 1300	3.54×10^{8}	3.84	.20	424.9	40.9	0.965
FeMnAl-I + FeMnAl-II	1300	$\exp(-16.6 - 0.86X)$[b]	3.40	0.16	------	-----	0.986
FeMnAl-II + FeMnAl-IIht	1300	3.30×10^{-8}	3.28	0.16	------	-----	0.985
Fe-40Al + Fe-40Al-ht + FeMnAl-II	1000 to 1100	$\exp(13.89 + 0.93Y)$[c]	5.92	0.25	438.3	27.3	0.959
Fe-40Al + Fe-40Al-ht + FeMnAl-II	1200	$\exp(-24.48 + 0.63Y)$[c]	4.38	0.15	------	-----	0.987
Fe-40Al + Fe-40Al-ht + FeMnAl-II	1300	$\exp(-18.14 + 0.99Y)$[c]	3.24	0.20	------	-----	0.968

[a] 1200 K to 2.15×10^{-7} s^{-1} and 1300 K to 2.15×10^{-7} s^{-1} values were not used in the fit.

[b] $X = 0$ for FeMnAl-I and $X = 1$ for FeMnAl-II.

[c] $Y = 0$ for the combined Fe-40Al alloys and $Y = 1$ for Fe-15Mn-40Al.

TABLE IV.—GRAIN SIZE OF THE FEAL-BASED ALLOYS DETERMINED AFTER ELEVATED TEMPERATURE COMPRESSIVE DEFORMATION.

Deformation conditions			Fe-40Al	Fe-40Al-ht	FeMnAl-II	FeMnAl-IIht
Temperature, K	Strain rate, s^{-1}	~Strain, percent	Grain Size, μm			
1000	2.2×10^{-4}	25	5	7.5	5.5	-----
1000	2.2×10^{-5}	12	-----	11	----	11
1000	2.2×10^{-6}	15	6	-----	6.5	-----
1000	2.2×10^{-7}	10	-----	10	6	10
1100	2.2×10^{-4}	25	6.5	10	7	10
1100	2.2×10^{-6}	13	9	10	7.5	-----
1100	2.2×10^{-7}	10	-----	12.5	10	12
1200	2.2×10^{-4}	25	9	11.5	9	12
1200	2.2×10^{-6}	13	12	13	9.5	[a]11.5
1200	2.2×10^{-7}	10	-----	19	14	11
1300	2.2×10^{-4}	25	11.5	17	18	15
1300	2.210^{-5}	13	-----	-----	15	14
1300	2.2×10^{-6}	13	13.5	16	18.5	[b]15
1300	2.2×10^{-7}	10	-----	-----	18.5	17.5

[a]20 percent deformation.
[b]17 percent deformation.

TABLE V.—TEMPERATURE COMPENSATED POWER LAW DESCRIPTIONS OF THE FLOW STRESS-STRAIN RATE-TEMPERATURE BEHAVIOR FOR IRON ALUMINIDES.

FeAl Composition	B (A), s^{-1}	p	δp	n	δn	Q, kJ/mol	δ_Q, kJ/mol	R_d^2
All	2.51×10^{7}	-----	-----	3.87	0.19	389.9	19.8	0.792
	1.15×10^{3}	2.04	0.14	5.65	0.17	404.5	11.9	0.926
	$\exp(9.055 + 1.87X)$[a]	2.48	0.14	5.86	0.15	448.7	12.4	0.945
Fe-39.8.Al	1.06×10^{6}	-----	------	3.33	0.27	363.6	32.6	0.772
	1.10×10^{3}	1.85	0.19	5.18	0.24	381.5	18.3	0.930
	$\exp(11.32 + 1.90X)$[a]	2.27	0.19	5.60	0.23	456.3	24.3	0.950

[a]$X = 0$ for the grain sizes ≥9 μm and $X = 1$ for grain sizes <9 μm.

TABLE VI.—COMPARISON OF THE ESTIMATED STRENGTH OF FEAL AS A FUNCTION OF GRAIN SIZE TO DATA FROM FEAL-BASED ALLOYS FROM THE LITERATURE.

Composition, at%	Grain size, μm	Temperature, K	Strain rate, s^{-1}	Strength, MPa	Source
Binary FeAl	100	1073	5×10^{-4}	44	eq. (4)
	40	↓	↓	65	eq. (4)
	10	↓	↓	117	eq. (4)
Fe-40Al-0.2Mo-0.05Zr-0.45C-0.02B	NR[a]	↓	↓	[b]96	(ref. 11)
Fe-40Al-0.5Mo-0.1Zr-1Ti-0.2C-0.02B	100	↓	↓	[b]150	(ref. 11)
Fe-39.6Al-0.2Mo-0.1Zr-0.4C-0.02B	22	↓	1×10^{-3}	[c]150	(ref. 12)
Fe-40Al-0.1Zr-0.4B	9	1100	2.5×10^{-4}	[d]140	(ref. 13)
Fe-38.5Al-0.2Mo-0.05Zr-0.13C	As-Cast, >100	1073	NR[a]	90	(ref. 14)
Fe-38.5Al-0.2Mo-0.05Zr-0.13C	10	1073	NR[a]	[c]210	(ref. 14)

[a]NR = not reported.
[b]Densified by hot extrusion, heat treated for 2 hr at 1373 K.
[c]Extruded at 1373 K.
[d]Extruded at 1250 K.

APPENDIX A.—COMPOSITIONS, INITIAL GRAIN SIZE, TEMPERATURE, FLOW STRESS, AND STRAIN RATE DATA FOR SEVERAL FEAL BASED ALLOYS FROM (REFS. 8 AND 9) AND THIS STUDY.

Al content, at%	Initial grain size, μm	Test temperature, K	Flow stress, MPa	Strain rate, s^{-1}
48.7	39	1100	29.5	2.2×10^{-5}
		1100	19.1	2.31×10^{-6}
		1100	13.65	2.2×10^{-7}
		1200	14.5	2.35×10^{-5}
		1200	10.25	2.4×10^{-6}
		1200	7.8	2.3×10^{-7}
		1300	16.3	1.91×10^{-3}
		1300	11.1	1.86×10^{-4}
		1300	9.3	2.28×10^{-5}
		1300	6.5	2.3×10^{-6}
48.2	41	1200	14.5	2.47×10^{-5}
		1200	10.6	2.43×10^{-6}
		1200	7.5	2.3×10^{-7}
		1300	17	1.87×10^{-3}
		1300	11.4	1.95×10^{-4}
		1300	8.2	1.78×10^{-5}
		1300	6.45	2.45×10^{-6}
		1400	6.8	2.31×10^{-4}
		1400	4.6	1.8×10^{-5}
		1400	3.1	2.34×10^{-6}
47.5	36	1100	32	2.33×10^{-5}
		1100	20.7	2.31×10^{-6}
		1100	15.5	2.28×10^{-7}
		1200	14.6	2.33×10^{-5}
		1200	10.8	2.45×10^{-6}
		1200	7.75	2.32×10^{-7}
		1300	17.4	1.87×10^{-3}
		1300	11.8	1.96×10^{-4}
		1300	8.75	1.77×10^{-5}
		1300	8.75	2.19×10^{-5}
		1300	5.7	1.8×10^{-6}
46.8	35	1200	16.3	2.33×10^{-5}
		1200	11.2	2.4×10^{-6}
		1200	7.5	2.31×10^{-7}
		1300	16.8	1.69×10^{-3}
		1300	16.5	1.87×10^{-3}
		1300	12.3	2.33×10^{-4}
		1300	9	1.9×10^{-5}
		1300	6.75	2.33×10^{-6}
		1400	8	2.08×10^{-4}
		1400	5.2	2.06×10^{-5}

APPENDIX A.—Continued.

Al content, at%	Initial grain size, μm	Test temperature, K	Flow stress, MPa	Strain rate, s^{-1}
45.7	19	1200	17.9	2.28×10^{-5}
		1200	12.5	2.4×10^{-6}
		1200	9	2.29×10^{-7}
		1300	24.7	2.00×10^{-3}
		1300	17.9	1.97×10^{-4}
		1300	14	1.97×10^{-5}
44.55	39	1200	17.8	2.35×10^{-5}
		1200	11.8	2.4×10^{-6}
		1200	8.6	2.33×10^{-7}
		1300	12.7	2.04×10^{-4}
		1300	8.7	1.98×10^{-5}
		1300	6.3	2.38×10^{-6}
		1300	6.4	2.00×10^{-6}
		1300	5.25	2.34×10^{-7}
		1400	5.5	2.00×10^{-5}
43.2	20	1200	20.2	2.43×10^{-5}
		1200	12.8	2.38×10^{-6}
		1200	8.75	2.23×10^{-7}
		1300	21	2.55×10^{-3}
		1300	17.5	1.84×10^{-4}
		1300	12.8	1.82×10^{-5}
		1400	11	2.05×10^{-4}
41.7	43	1200	18.7	2.32×10^{-5}
		1200	11.7	2.33×10^{-6}
		1200	8.35	2.3×10^{-7}
		1300	18.9	1.97×10^{-3}
		1300	12.6	2.1×10^{-4}
		1300	8.7	1.9×10^{-5}
		1300	9	2.35×10^{-5}
		1300	6.1	2.00×10^{-6}
		1300	4	2.31×10^{-7}
		1400	9.6	2.33×10^{-4}
		1400	6.1	1.99×10^{-5}
		1400	3.9	1.97×10^{-6}

APPENDIX A.—Continued.

Al content, at%	Initial grain size, μm	Test temperature, K	Flow stress, MPa	Strain rate, s^{-1}
39.8	185	1200	10.2	2.16×10^{-5}
		1200	6.3	2.21×10^{-6}
		1200	4.15	2.17×10^{-7}
		1300	4.45	2.31×10^{-5}
		1300	2.75	2.26×10^{-6}
		1300	1.95	2.18×10^{-7}
		1400	3.7	2.42×10^{-4}
		1400	2.3	2.35×10^{-5}
		1400	1.9	2.29×10^{-6}
		1400	1.45	2.23×10^{-6}
		1400	0.85	2.1×10^{-7}
39.8	55	1200	19.45	2.05×10^{-4}
		1200	14.2	1.78×10^{-5}
		1200	7.7	1.8×10^{-6}
		1200	5.75	2.16×10^{-7}
		1300	10.4	2.03×10^{-4}
		1300	7	1.77×10^{-5}
		1300	5.2	1.8×10^{-6}
		1400	3.65	2.14×10^{-5}
		1400	3.4	2.24×10^{-6}
		1400	2.9	2.33×10^{-6}
39.8	11	1200	37.4	2.67×10^{-4}
		1200	26.6	2.38×10^{-5}
		1300	33.2	2.6×10^{-3}
		1300	24	2.6×10^{-4}
39.8	9	1200	39.6	2.75×10^{-4}
		1200	28.7	2.35×10^{-5}
		1300	33.9	2.78×10^{-3}
		1300	24.2	2.6×10^{-4}
39.8	6.5	1000	169.3	2.01×10^{-4}
		1000	121.2	2.08×10^{-5}
		1000	78.8	2.22×10^{-6}
		1000	52.4	2.32×10^{-7}
		1100	66.6	2.04×10^{-4}
		1100	47.5	2.05×10^{-5}
		1100	31.1	2.09×10^{-6}
		1100	19.5	2.14×10^{-7}

APPENDIX A.—Concluded.

Al content, at%	Initial grain size, μm	Test temperature, K	Flow stress, MPa	Strain rate, s^{-1}
39.8	5.5	1000	142.4	2.16×10^{-4}
		1000	105.6	2.17×10^{-5}
		1000	75.4	2.18×10^{-6}
		1000	58.8	2.18×10^{-7}
		1100	112.5	2.03×10^{-3}
		1100	76.7	2.17×10^{-4}
		1100	54.4	2.18×10^{-5}
		1100	38.7	2.17×10^{-6}
		1100	36.7	2.16×10^{-6}
		1100	29.5	2.18×10^{-7}
		1100	24.5	2.16×10^{-7}

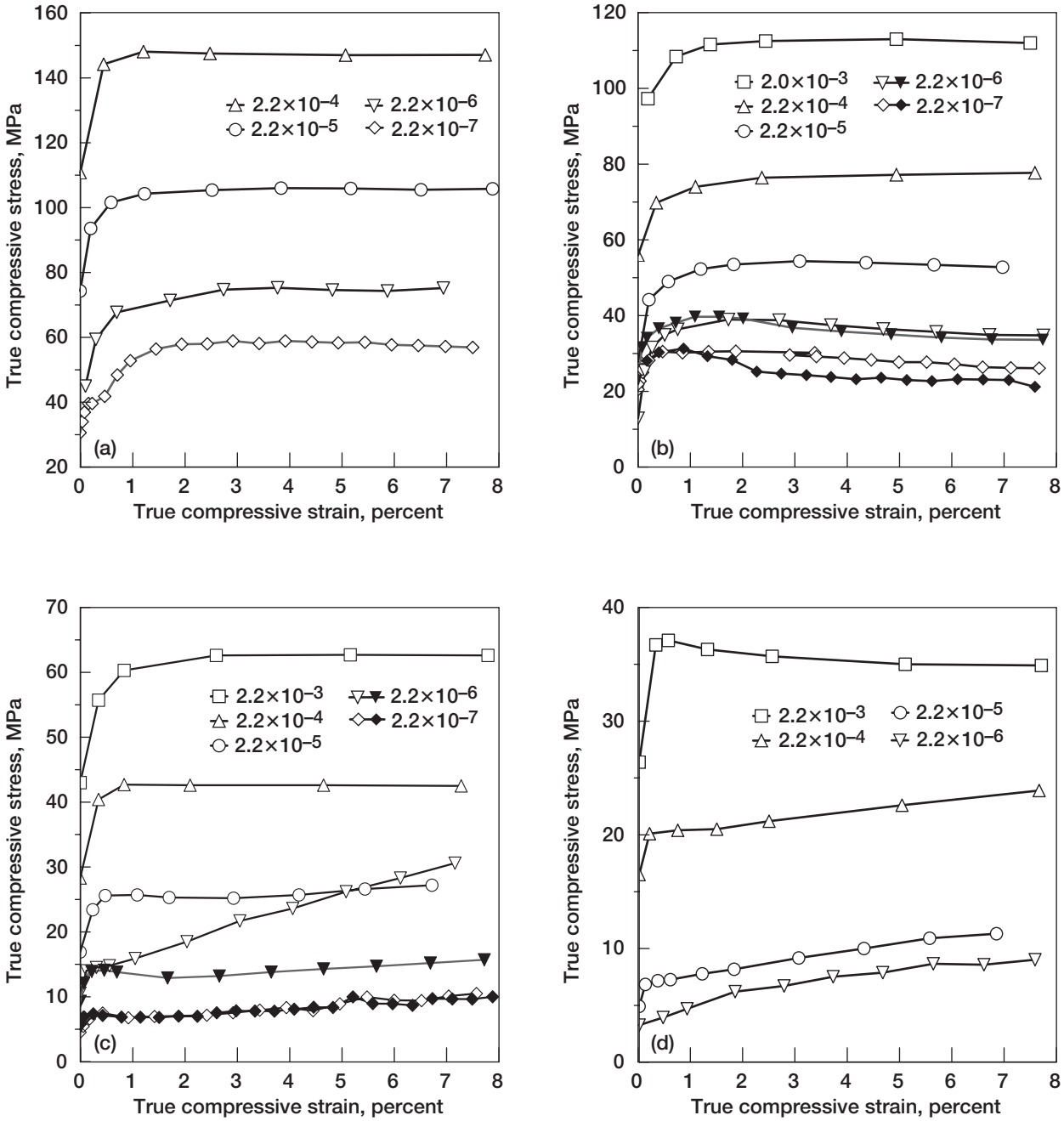

Figure 1.—True compressive stress-strain curves as functions of nominal strain rate and temperature for 1000 K as-extruded Fe-39.8Al (Fe-40Al). Filled symbols indicate nominally duplicate tests.

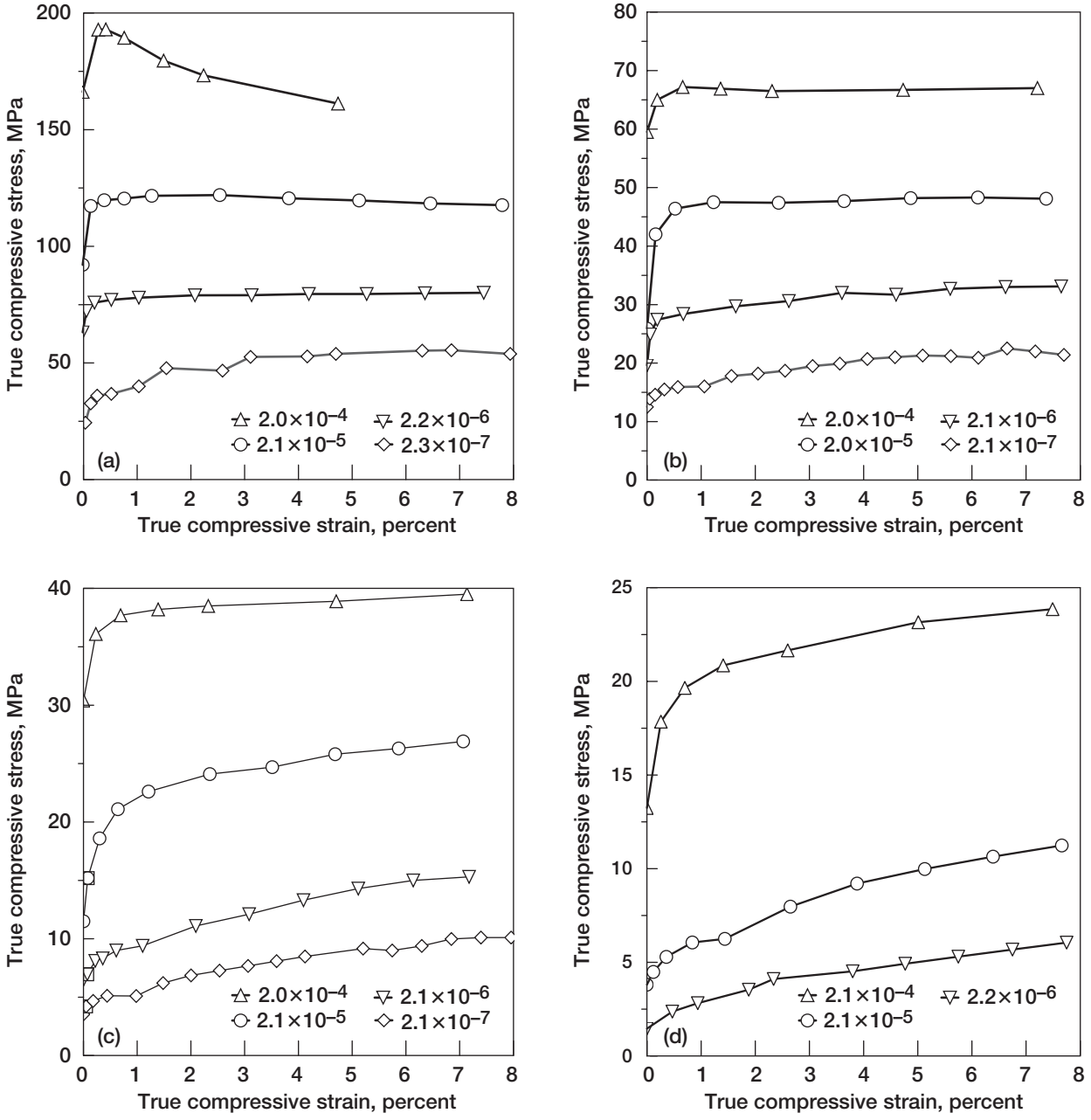

Figure 2.—True compressive stress-strain curves as functions of nominal strain rate and temperature for Fe-39.8Al after 1000 K extrusion and a 16 h at 1200 K heat treatment (Fe-40Al-ht).

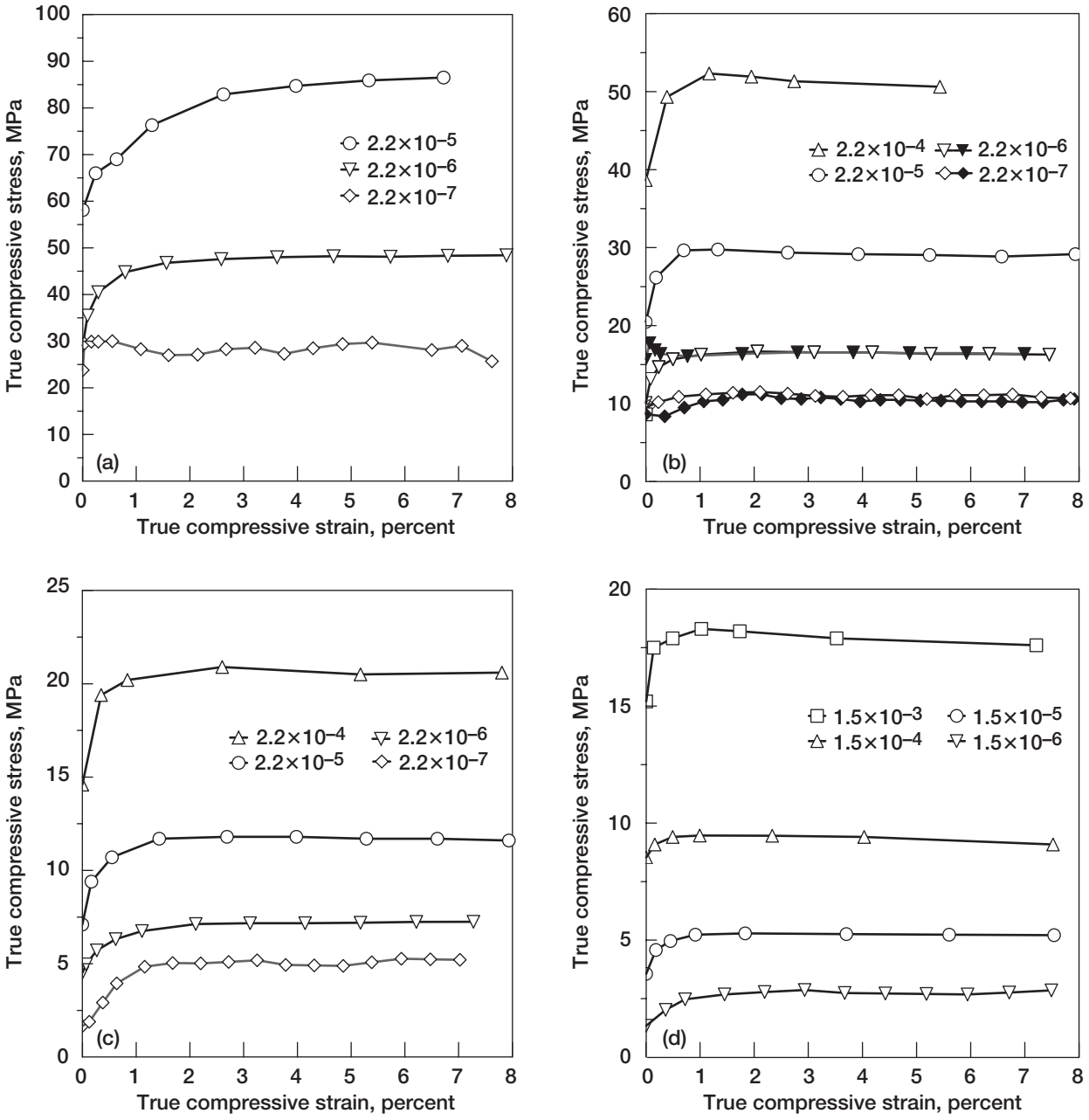

Figure 3.—True compressive stress-strain curves 1505 K compacted and extruded Fe-15.6Mn-39.4Al (FeMnAl-I) as functions of nominal strain rate and temperature. Filled symbols indicate nominally duplicate tests.

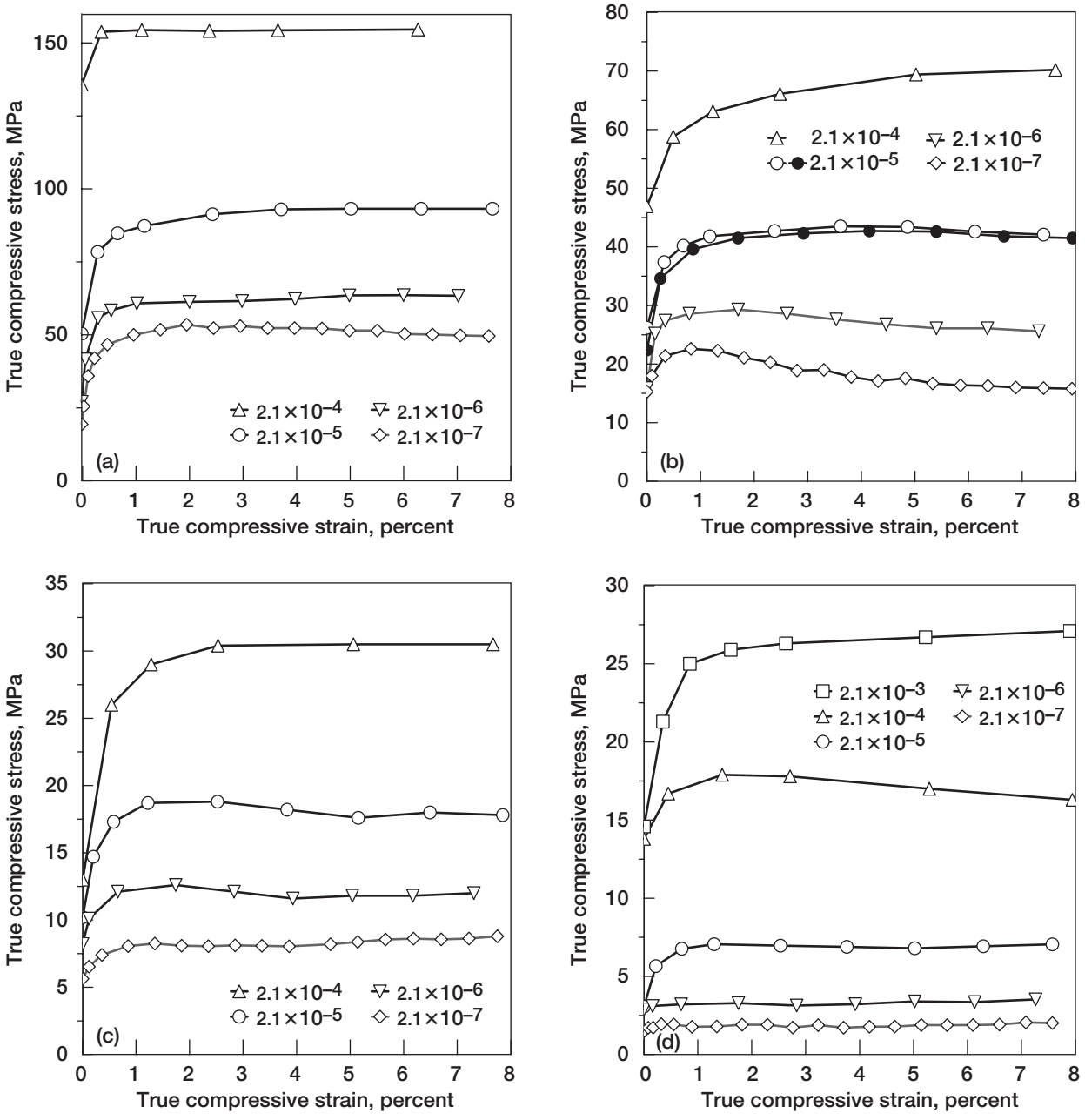

Figure 4.—True compressive stress-strain curves for 1100 K as-extruded Fe-15.6Mn-39.4Al (FeMnAl-II) as functions of nominal strain rate and temperature. Filled symbols indicate nominally duplicate tests.

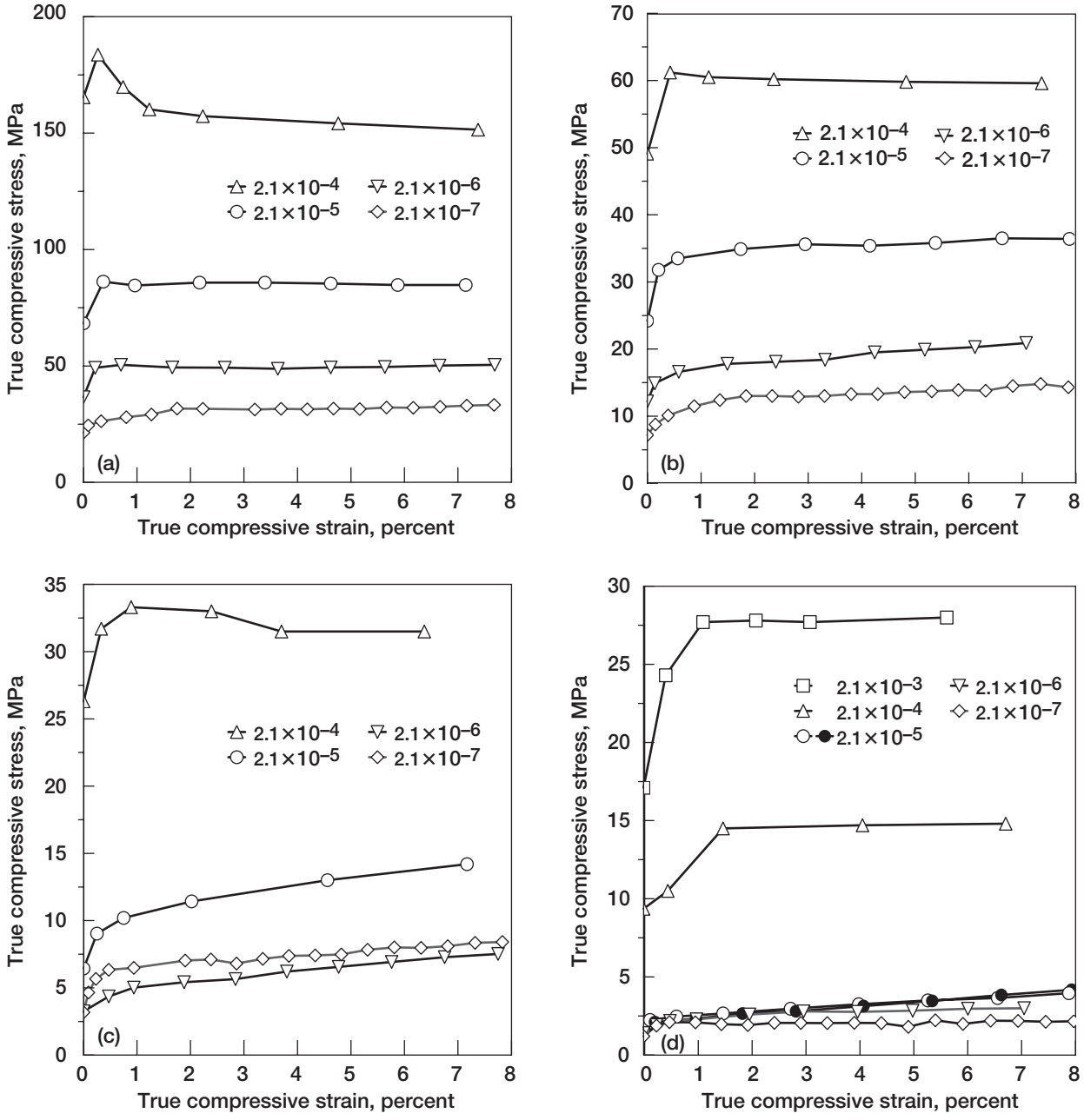

Figure 5.—True compressive stress-strain curves for Fe-15.6Mn-39.4Al after 1100 K extrusion and a 16 h at 1300 K heat treatment (FeMnAl-IIht) as functions of nominal strain rate and temperature. Filled symbols indicate nominally duplicate tests.

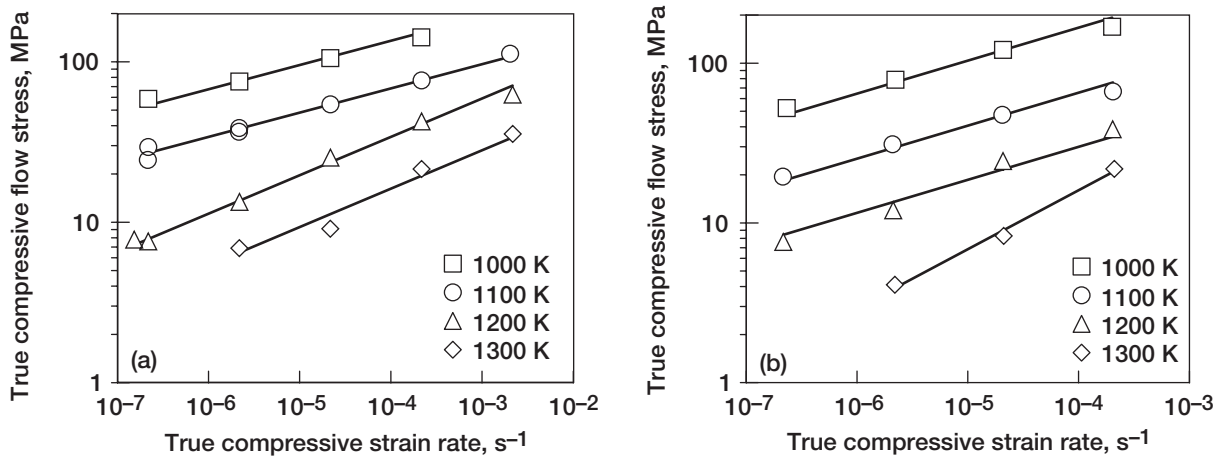

Figure 6.—True compressive flow stress-strain rate-temperature behavior for (a) Fe-40Al and (b) Fe-40Al-ht.

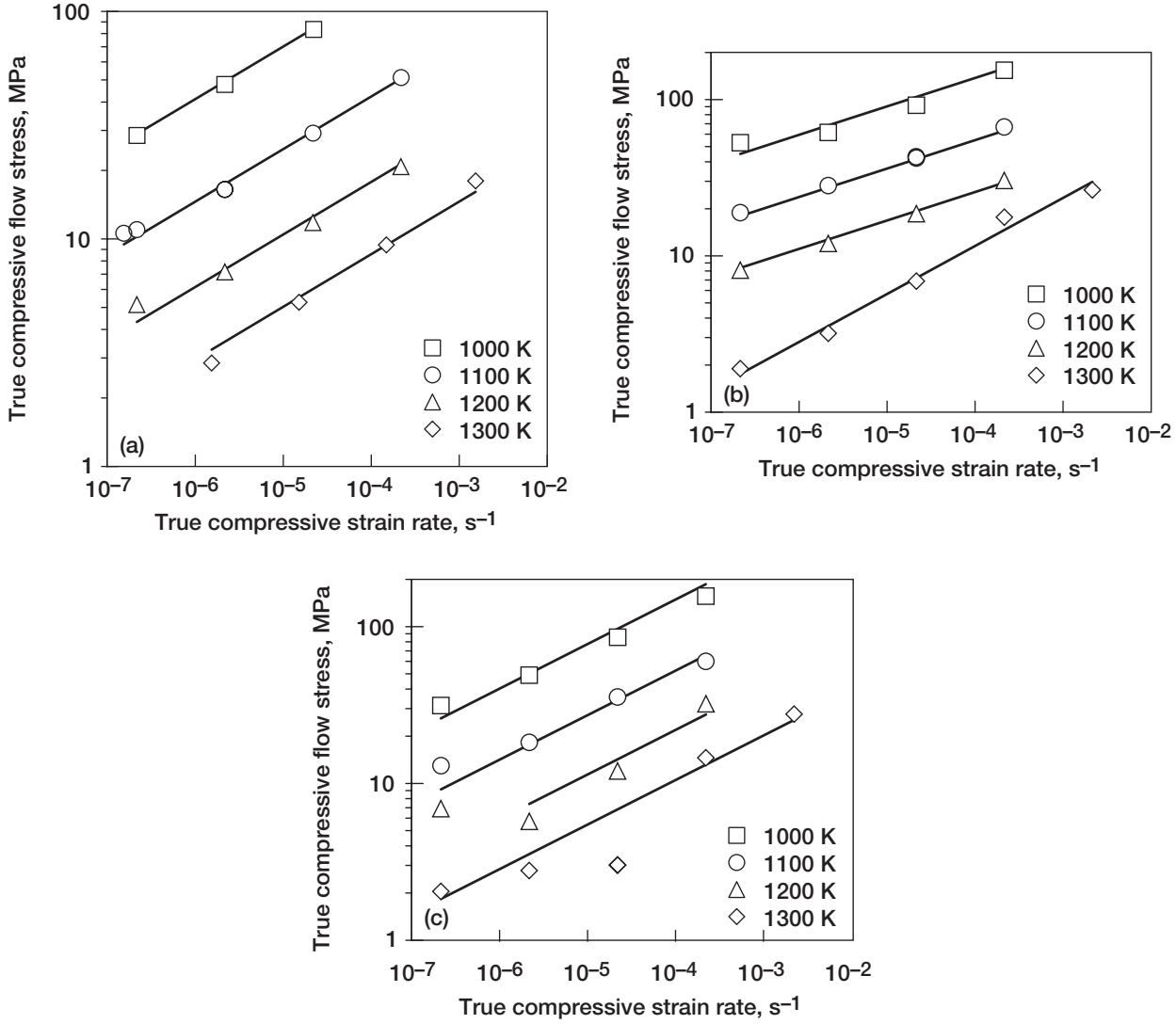

Figure 7.—True compressive flow stress-strain rate-temperature behavior for (a) FeMnAl-I, (b) FeMnAl-II, (c) FeMnAl-IIht.

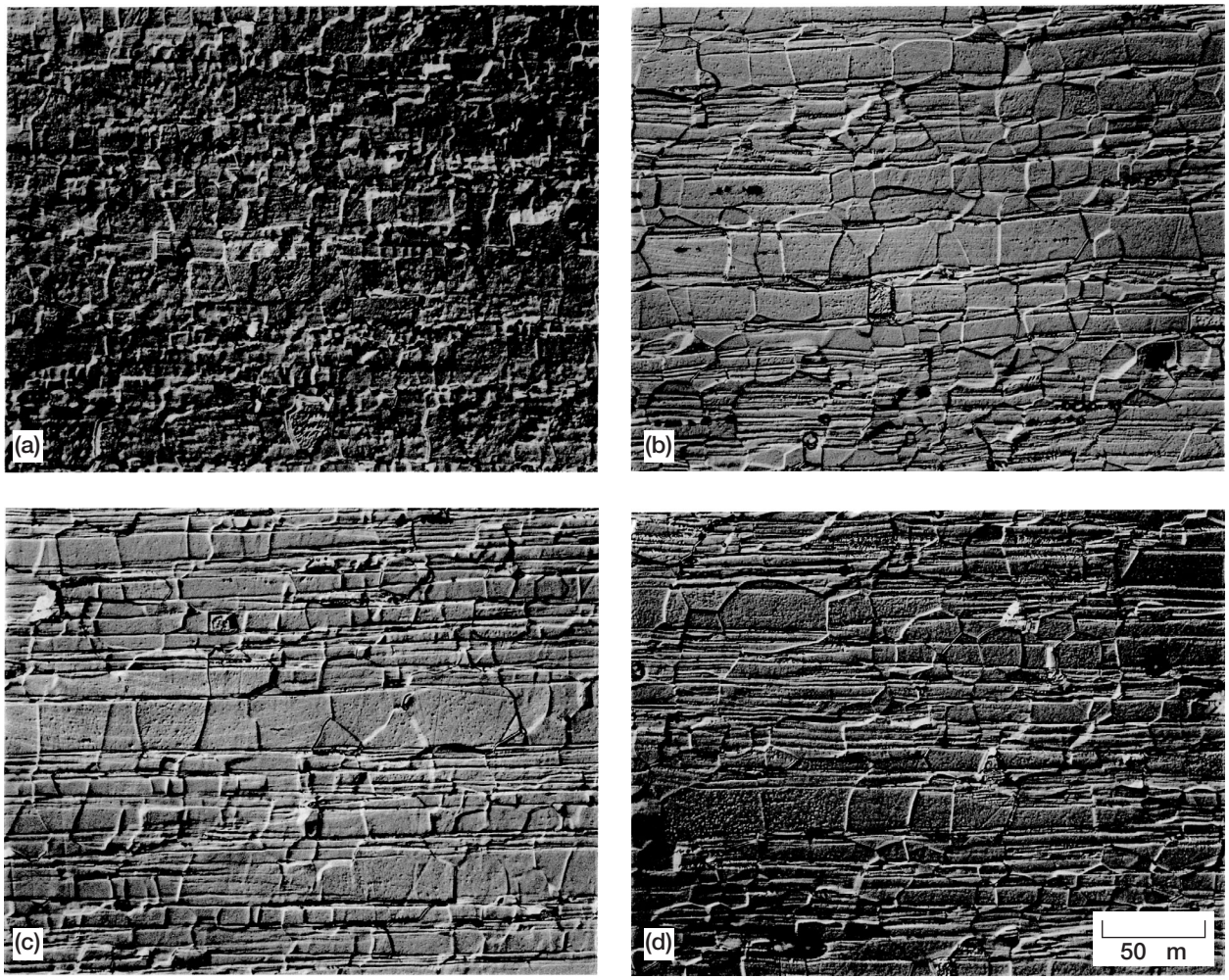

Figure 8.—Microstructure of Fe-39.8Al compression tested under constant velocity conditions. The extrusion axis and compression direction are horizontal in all parts; samples were etched and photographed under DIC. Fe-40Al (a) at 1100 K and 2.2×10^{-4} s^{-1} to 26.6 percent and (b) at 1300 K and 2.2×10^{-6} s^{-1} to 13 percent; Fe-40Al-ht (c) at 1100 K and 2.2×10^{-4} s^{-1} to 25.4 percent and (d) at 1300 K and 2.2×10^{-6} s^{-1} to 12 percent.

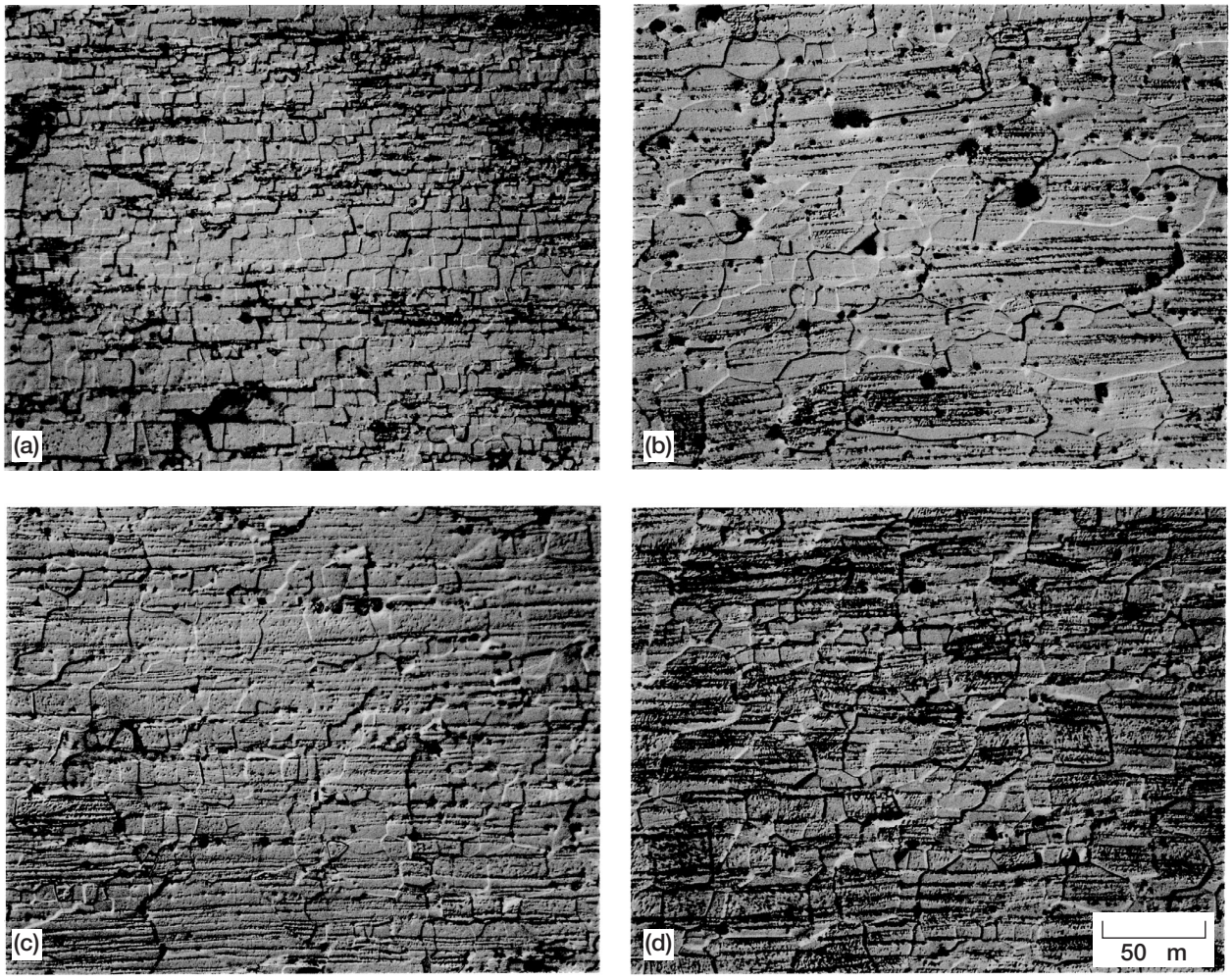

Figure 9.—Microstructure of Fe-15.6Mn-39.4Al compression tested under constant velocity conditions. The extrusion axis and compression direction are horizontal in all parts; samples were etched and photographed under DIC. FeMnAl-II (a) at 1000 K and 2.2×10^{-7} s^{-1} to 9.5% and (b) at 1300 K and 2.2×10^{-7} s^{-1} to 9.4%; FeMnAl-IIht (c) at 1000 K and 2.2×10^{-7} s^{-1} to 9.4% and (d) at 1300 K and 2.2×10^{-5} s^{-1} to 15%.

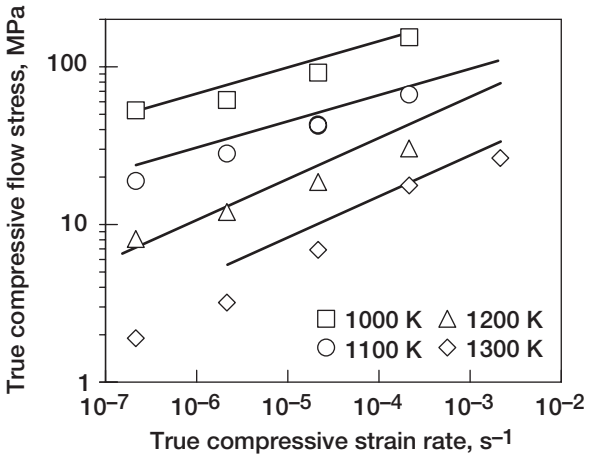

Figure 10.—Comparison of true compressive flow stress-strain rate-temperature behavior for as 1100 K extruded FeMnAl-II (data points) to the predicted behavior of joined (a) Fe-40Al and Fe-40Al-ht (curves).

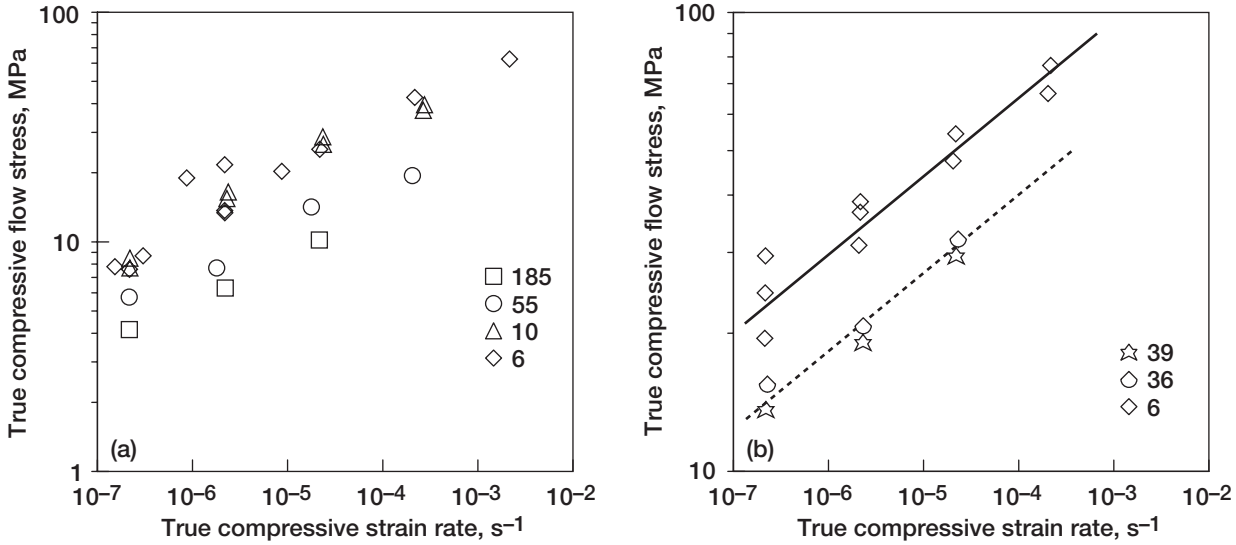

Figure 11.—Flow stress-strain rate results for iron aluminides as a function of initial grain size in microns (a) for Fe-39.8Al at 1200 K and (b) for Fe-39.8Al (~6 μm). Fe-48.7Al (39 μm) and Fe-47.5Al (36 μm) at 1100 K, where the curves illustrate the predicted behavior for 40 and 6 micron grain size alloys from eq. (3).

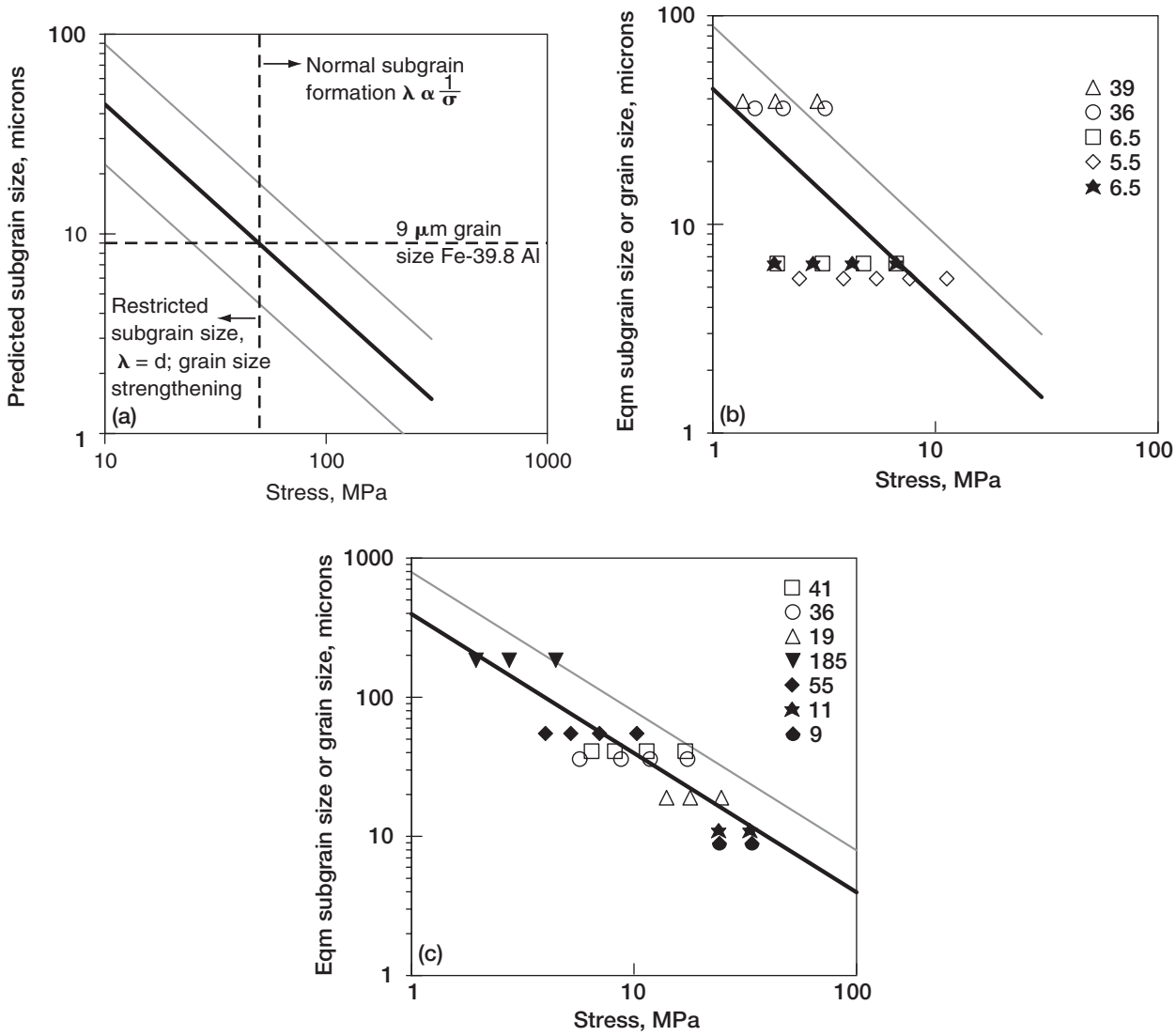

Figure 12.—(a) Predicted equilibrium subgrain sizes for Fe-40Al at 1100 K as a function of stress, where the upper and lower gray curves are twice and half, respectively, the predicted values; (b) comparison of the 1100 K flow stress-initial grain size data for several alloys to the predicted subgrain size for Fe-40Al at 1100 K: open symbols are for Fe-48.7Al = 39 μm; Fe-47.5Al = 36 μm; and Fe-39.8Al = 6.5 and 5.5 μm and solid symbols are for FeMnAl-II = 6.5 μm; (c) comparison of the observed 1300 K flow stress-initial grain size data for several binary FeAl alloys to the predicted subgrain size for Fe-40Al at 1300 K, where

Composition, % Al	Initial grain size, μm	Range in strain rates, s^{-1}
48.2	41	$2.5\times10^{-6} - 1.9\times10^{-3}$
47.5	36	$1.8\times10^{-6} - 1.9\times10^{-3}$
45.7	19	$2.0\times10^{-5} - 2.0\times10^{-3}$
39.8	185	$2.2\times10^{-7} - 2.3\times10^{-5}$
39.8	55	$1.7\times10^{-7} - 2.0\times10^{-4}$
39.8	11	$2.6\times10^{-4} - 2.6\times10^{-3}$
39.8	9	$2.6\times10^{-4} - 2.8\times10^{-3}$

REPORT DOCUMENTATION PAGE

Form Approved
OMB No. 0704-0188

1. AGENCY USE ONLY (*Leave blank*)	2. REPORT DATE	3. REPORT TYPE AND DATES COVERED
	March 2004	Technical Memorandum

4. TITLE AND SUBTITLE

Elevated Temperature Deformation of Fe-39.8Al and Fe-15.6Mn-39.4Al

5. FUNDING NUMBERS

WBS–22–708–31–04

6. AUTHOR(S)

J. Daniel Whittenberger

7. PERFORMING ORGANIZATION NAME(S) AND ADDRESS(ES)

National Aeronautics and Space Administration
John H. Glenn Research Center at Lewis Field
Cleveland, Ohio 44135–3191

8. PERFORMING ORGANIZATION REPORT NUMBER

E–14237–1

9. SPONSORING/MONITORING AGENCY NAME(S) AND ADDRESS(ES)

National Aeronautics and Space Administration
Washington, DC 20546–0001

10. SPONSORING/MONITORING AGENCY REPORT NUMBER

NASA TM—2004-212947

11. SUPPLEMENTARY NOTES

J. Daniel Whittenberger (retired) NASA Glenn Research Center. Responsible person, Mike Nathal, organization code 5120, 216–433–9516.

12a. DISTRIBUTION/AVAILABILITY STATEMENT

Unclassified - Unlimited
Subject Category: 26 Distribution: Nonstandard

Available electronically at http://gltrs.grc.nasa.gov

This publication is available from the NASA Center for AeroSpace Information, 301–621–0390.

12b. DISTRIBUTION CODE

13. ABSTRACT ***(Maximum 200 words)***

The elevated temperature compressive properties of binary Fe-39.8 at% Al and Fe-15.6Mn-39.4Al have been measured between 1000 and 1300 K at strain rates between 10^{-7} and 10^{-3} s^{-1}. Although the Mn addition to iron aluminide did not change the basic deformation characteristics, the Mn-modified alloy was slightly weaker. In the regime where deformation of FeAl occurs by a high stress exponent mechanism ($n \approx 6$), strength increases as the grain size decreases at least for diameters between ~200 and ~10 μm. Due to the limitation in the grain size-flow stress-temperature-strain rate database, the influence of further reductions of the grain size on strength is uncertain. Based on the appearance of subgrains in deformed iron aluminide, the comparison of grain diameters to expected subgrain sizes, and the grain size exponent and stress exponent calculated from deformation experiments, it is believed that grain size strengthening is the result of an artificial limitation on subgrain size as proposed by Sherby, Klundt and Miller [*Met. Trans A*. **8A** (1977) 843–50].

14. SUBJECT TERMS

Intermetallic; Creep; Elevated temperature; Plastic deformation; Models

15. NUMBER OF PAGES

34

16. PRICE CODE

17. SECURITY CLASSIFICATION OF REPORT	18. SECURITY CLASSIFICATION OF THIS PAGE	19. SECURITY CLASSIFICATION OF ABSTRACT	20. LIMITATION OF ABSTRACT
Unclassified	Unclassified	Unclassified	